Phase Behavior of Styrene−Isoprene Diblock Copolymers in Strongly Selective Solvents

Chiajen Lai,[†,§] William B. Russel,[‡] and Richard A. Register*[,‡]

Department of Chemical Engineering and Princeton Materials Institute, Princeton University, Princeton, New Jersey 08544

Received September 28, 2001; Revised Manuscript Received November 15, 2001

ABSTRACT: The phase behavior of polystyrene−polyisoprene diblock copolymers diluted with solvents strongly selective for polyisoprene was investigated using variable-temperature small-angle X-ray scattering. Tetradecane was employed as a model selective solvent; its addition induced lyotropic order−order transitions, with as many as five ordered phases found in solutions of one diblock as tetradecane content was varied. The mesophases observed for tetradecane solutions of 10 different diblocks can be partially collapsed into a single two-dimensional map of segregation strength vs overall polystyrene content, as if the selective solvent simply alters the volume fraction of the soluble block. Among strongly selective solvents (tetradecane, tributylamine, squalane), measurable and even large differences in diblock−solvent phase behavior are revealed, in both the locations of lyotropic order−order transitions and the thermotropic order−disorder transition. The addition of squalane to polystyrene-rich diblocks actually elevates the order−disorder transition temperature relative to the diblock melt.

Introduction

The phase behavior of block copolymer melts has been studied extensively, due to the fascinating nanometer-scale structures (such as spheres, cylinders, gyroid, and lamellae) into which these materials spontaneously self-assemble.[1,2] When the repulsive interblock interactions are sufficiently weakened, such as through an increase in temperature, block copolymers undergo an order−disorder transition (ODT).[1,2] Reversible thermotropic transitions between different ordered structures were first reported in the early 1990s,[3−7] and while numerous reports have followed, such thermotropic order−order transitions (OOTs) are nonetheless relatively uncommon. Most diblocks show only one ordered phase over the accessible temperature range (typically bounded by a glass transition on the low end and either by the ODT or by degradation on the high end); only selected diblocks show two equilibrium ordered phases, and reports of diblocks exhibiting three phases are rare.[3] By contrast, the addition of a second component, such as a solvent or low-molecular-weight homopolymer, can greatly enrich the phase behavior as compared with the simple diblock melt, due to the possibility of both lyotropic and thermotropic transitions.[8]

The phase behavior of diblock−solvent mixtures depends strongly on the affinity of the solvent for the two blocks, A and B. Solvents that are good for both blocks partition roughly uniformly across the A-rich and B-rich domains, with some enhancement near the domain interfaces;[9] perfectly equal partitioning defines the ideal neutral solvent. The addition of a neutral solvent is qualitatively equivalent to raising the temperature; sufficient solvent will push the system into the disordered state, but in most cases addition of a neutral solvent will not induce an order−order transition.[9−11] When the added solvent is instead a poor solvent or nonsolvent for one of the blocks (and a good solvent for the other), lyotropic order−order transitions are easily induced by the unequal partitioning of solvent across the A-rich and B-rich domains, which alters their relative volume fractions. If the solvent is so poor for the A block that the A-rich domains imbibe little solvent, then not only will microphase separation persist to high dilutions, but the A-rich domains will also retain a glass transition temperature similar to that in the undiluted diblock. These facts have been exploited commercially for well over a decade in the form of thermoplastic elastomer gels, which comprise a polystyrene−(poly(ethylene-*co*-butene))−polystyrene triblock copolymer highly diluted with an aliphatic oil (a nonsolvent for polystyrene).[12−14] For diblock copolymers, high dilution with a B-selective solvent typically leads to micellization, with the micelle cores formed by the insoluble A-rich regions.[15−17]

Block copolymer phase behavior in selective solvents has only recently been treated theoretically outside this dilute micellar limit. While the mean-field phase behavior of diblocks of a particular chemistry (i.e., identity of A and B) can be described in a two-dimensional map of segregation strength χN vs diblock composition (e.g., volume fraction of A block),[18] the addition of a particular solvent adds concentration (e.g., polymer weight fraction W_P) as a third parameter. Moreover, the effect that this solvent has on the phase behavior depends on the strengths of the segmental interactions between the three species present, i.e., χ_{AB}, χ_{AS}, and χ_{BS}, where "S" indicates solvent. Banaszak and Whitmore[19] presented the first self-consistent mean-field (SCMF) theory for such systems, restricted to block copolymer solutions exhibiting the lamellar mesophase in selective solvents. Recently, Huang and Lodge[20] presented a SCMF approach for diblocks in selective solvents that treats all the "classical" phases (spheres, cylinders, lamellae). Though this treatment retains Gaussian statistics for polymer in solution, thus neglecting chain swelling, it successfully captures two key features: dilution-induced transitions between the classical phases as solvent

† Department of Chemical Engineering.
‡ Princeton Materials Institute.
§ Present address: Bristol-Myers Squibb Pharmaceutical Research Institute, P.O. Box 191, New Brunswick, New Jersey 08903.
* To whom correspondence should be addressed. E-mail register@princeton.edu.

10.1021/ma011696z CCC: $22.00
Published on Web 12/21/2001

selectivity is increased and stabilization of the ordered structures relative to solutions of identical diblock concentration in a neutral solvent.

Though these principal features are now well-known, systematic experimental investigations of the phase behavior of diblock copolymers in selective solvents—where diblock composition, solvent content, and temperature are varied—are few indeed, especially for more concentrated solutions where a range of ordered phases is expected. The rich phase behavior of block copolymers of ethylene oxide and propylene oxide, in the presence of both water and oil, has been studied in some detail.[21] However, the strong temperature dependence of the solvent quality of water for poly(ethylene oxide) masks other temperature-induced effects. In simple hydrocarbon systems, the early work of Watanabe et al.[15] and of Shibayama et al.[22] showed that a polystyrene−polybutadiene (S/B) diblock, which formed polystyrene cylinders in bulk, instead formed spherical micelles with PS cores in the strongly PB-selective solvent tetradecane, with the micelles packed onto a body-centered-cubic (bcc) lattice. Later, McConnell et al.[17,23] studied the behavior of polystyrene−polyisoprene (S/I) diblocks covering a broad range of composition (S/I ratio) in decane, a nonsolvent for PS; their focus was on relatively dilute solutions, which exhibited spherical micelles packed into either bcc or face-centered-cubic (fcc) lattices. Most recently, Hanley et al.[24] have presented the phase diagrams for a single S/I diblock in two moderately PS-selective solvents (dibutyl phthalate, DBP; diethyl phthalate, DEP) and a strongly PI-selective solvent (tetradecane, TD). These diagrams showed the anticipated lyotropic transitions between different ordered phases as well as some unexpected features, such as coexistence between different ordered phases.

Here, our objective is to systematically examine the phase behavior of S/I diblocks diluted in strongly selective solvents, beginning with TD. Solvent content and temperature are varied to elucidate the diagram for each diblock in TD; then diagrams for diblocks of different composition (PS content) are collapsed together into a map exhibiting the general features of the well-known melt phase map. Finally, the phase behavior of selected diblocks in two other strongly PS-selective solvents is examined and compared and contrasted with the behavior in TD and in a neutral solvent.

Experimental Section

Diblock Synthesis and Characterization. Polystyrene−polyisoprene (S/I) diblock copolymers were either provided by DEXCO Polymers or synthesized by the authors for this study, so as to span a wide range of compositions with accessible ODTs. All polymers were synthesized via sequential anionic polymerization in hydrocarbon solvent, PS block first, using *sec*-butyllithium as initiator. Compositions (weight fraction of polystyrene in diblock, W_S) were determined by ^{1}H NMR in $CDCl_3$; all the I blocks are high (93%) in 1,4-addition. Several replicate solutions of selected diblocks were prepared for NMR analysis, which allowed us to set a precision of ±0.2 wt % on the compositions so determined. True molecular weights (Table 1) and polydispersities (<1.05 for all polymers) were determined via gel permeation chromatography (GPC) in toluene, using narrow-distribution PS and PI standards. When a sample of the first block in the diblock was available, its molecular weight was used in conjunction with the diblock's composition to calculate the diblock molecular weight; otherwise, the method described by Sebastian and Register[25] was used. Diblocks are identified as S/I *m*/*n*, where *m* and *n* are the approximate weight-average molecular weight (M_w) values of the PS and PI blocks in kg/mol.

Table 1. Characteristics of the Bulk S/I Diblock Copolymers Employed

diblock	W_S	M_w (kg/mol)	bulk morphology	T_{ODT} (°C)
S/I 10/69	0.131	79.0	S_S	201
S/I 9/57	0.135	65.9	S_S	161
S/I 8/26	0.241	35.9	C_S	144
S/I 8/17	0.334	25.2	C_S	158
S/I 10/16	0.378	25.6	G_S	171
S/I 10/15	0.393	24.4	G_S	149
S/I 11/10	0.516	22.6	L	178
S/I 17/9	0.677	27.8	G_I	198
S/I 19/7	0.716	28.5	C_I	198
S/I 24/6	0.803	31.7	C_I	158

Since our aim here is to study diblock−solvent phase behavior, it was important that no PS homopolymer (formed by termination of the first block during polymerization) be present, especially as PS is insoluble in the selective solvents studied here. As synthesized, S/I 11/10 contained a small amount of terminated first block, which was removed via fractionation in toluene/methanol to yield pure block copolymer (PS homopolymer undetectable by GPC, <0.2 wt %) prior to characterization. The other polymers showed no detectable homopolymer, though we note that the detection limit for terminated first block in diblocks with $W_S > {}^2/_3$ is somewhat larger than 0.2 wt %, due to the modest difference in hydrodynamic volume between the first block and the diblock.

All materials contained either a commercial stabilizer package or 0.2 wt % butylated hydroxytoluene (relative to polymer) to forestall thermooxidative degradation. GPC on a 70 wt % solution of S/I 10/69 in squalane showed that even after 6 h of heating to temperatures as high as 170 °C, no degradation was detectable. While some solutions had even higher ODT temperatures, the T_{ODT} values were confirmed through a second heating run, indicating that any possible degradation did not significantly influence T_{ODT}.

Solution Preparation. A total of four solvents were employed in this work: 1,3,5-triisopropylbenzene, TIPB (bp 232 °C); tetradecane, TD (bp 252 °C); tri(*n*-butylamine), TBA (bp 216 °C); and squalane, SQ (bp 176 °C at 0.05 Torr). The low vapor pressures of these solvents led to negligible evaporation during testing. TIPB is a good solvent for both PS and PI, so solutions were simply made by mixing the appropriate quantities of S/I diblock and TIPB and heating at 120 °C under dry nitrogen until the solutions were macroscopically homogeneous. The same procedure was used to prepare more dilute (weight fraction of polymer $W_P < {}^1/_2$) diblock solutions in TD, TBA, or SQ, though higher temperatures were employed (140−160 °C). However, this approach did not produce homogeneous TD, TBA, or SQ solutions at $W_P \geq {}^1/_2$ in a reasonable time. Such concentrated TD and TBA solutions were prepared from solutions with $W_P \approx 0.4$ by slowly evaporating solvent under dynamic vacuum in an oven at 100−110 °C. Solution weight was repeatedly checked to produce the desired final W_P. This method could not be used to prepare concentrated solutions in SQ because of its extremely low vapor pressure, so instead a volatile cosolvent (cyclohexane) was added to the initial diblock−SQ mixture. The solutions were stirred at room temperature until homogeneous and then heated under flowing dry nitrogen at ~10 °C/h to 100 °C. The remaining traces of cyclohexane were removed at 110 °C under vacuum, as verified gravimetrically.

Measurement Techniques. SAXS data were acquired using a laboratory system described elsewhere,[26] employing a sealed tube source, a compact Kratky camera with a microprocessor-controlled hotstage,[27] and a one-dimensional position-sensitive detector. For melts, the camera was simply kept under dynamic vacuum, but for the solutions this led to detectable solvent evaporation at the highest temperatures. Instead, for the solutions, the camera was kept under a slight positive pressure of helium. Data were reduced using previously reported procedures[26] to desmeared absolute intensity vs the scattering vector $q = 4\pi \sin\theta/\lambda$, where λ is the Cu Kα

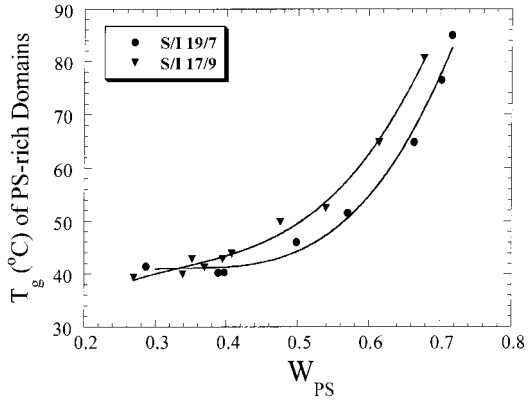

Figure 1. Glass transition temperatures (T_g) for the PS-rich domains in TD solutions of S/I 19/7 (●) and 17/9 (▼). Abscissa (W_{PS}) is the weight fraction of PS in the solution; the rightmost point in each set corresponds to the undiluted diblock. Continuous curves are guides to the eye.

radiation wavelength and 2θ is the scattering angle. ODT temperatures (T_{ODT}) were determined by SAXS following the method described in the Results and Discussion. T_{ODT} values for the melts, listed in Table 1 and with a precision of ±1 °C, all fall within a modest and easily accessible temperature range (144−201 °C). Several of these T_{ODT} values were confirmed independently via rheometry.[28] Once the ODT was roughly determined, samples were heated to above T_{ODT}, then cooled to approximately 40 °C, and then reheated in steps to determine the structure at each measurement temperature. Typical data acquisition times were 6 min, with 10 min allowed for equilibration following a temperature change.

A Perkin-Elmer DSC-7, cooled with liquid nitrogen and calibrated with indium and mercury or zinc, was used to measure the glass transition temperatures, T_g (midpoint of heat capacity rise), of the PS-rich domains in selected diblock melts and solutions. Data were acquired at 10 °C/min, and T_g values were determined on the second heat to eliminate physical aging in the PS-rich domains. For a few solutions, multiple DSC scans were run, yielding a standard deviation of ±3 °C in T_g.

Results and Discussion

Solvent Partitioning into Insoluble Domains. While tetradecane is a nonsolvent for PS, it is still possible that some TD will partition into the PS-rich domains. A quick way to assess how closely a solvent conforms to the "perfectly selective" ideal is to measure the glass transition temperature (T_g) of the domains formed by the insoluble block, which will be reduced by any imbibed solvent. Figure 1 shows the concentration dependence of the PS-rich domain T_g for PS−PI 19/7 and 17/9. For each data set, the rightmost point corresponds to bulk diblock, with a PS-domain $T_g \approx 83$ °C. As TD is added (total weight fraction of polystyrene in solution, W_{PS}, is decreased), the PS T_g initially drops steeply but then approaches a plateau, reflecting a saturation limit of the PS domains. These T_g values can be converted to weight fractions of TD through the use of models for the T_g of miscible systems. For the present purpose, an approximate figure is sufficient; both the Fox equation[29] (using the rule of thumb[30] that $T_g = T_m/2$ for TD, a symmetric molecule, where T_m is the melting temperature in absolute units) and the Chow equation[31] indicate that even for the most diluted systems in Figure 1, the PS-rich domains still contain less than 9 wt % TD at their T_g. This limited uptake of TD is consistent with literature reports for other styrenic block copolymers diluted with other aliphatic hydrocarbons[17,32] and suggests that TD does indeed approach this "perfectly selective" ideal and should thus be highly effective in inducing lyotropic order−order transitions.[24]

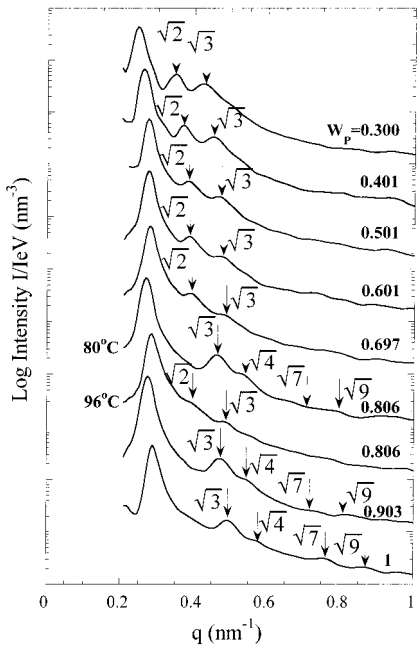

Figure 2. SAXS patterns for TD solutions of S/I 8/26 at various polymer weight fractions W_P. From bottom (bulk diblock) to top (most dilute solution), mesophase morphologies (W_P, T) are: C_S (1, 130 °C); C_S (0.903, 100 °C); S_S (0.806, 96 °C); C_S (0.806, 80 °C); S_S (0.697, 80 °C); S_S (0.601, 70 °C); S_S (0.501, 66 °C); S_S (0.401, 54 °C); S_S (0.300, 46 °C). Arrows indicate the positions of higher-order reflections characteristic of the mesophase structure. Profiles are shifted along the intensity axis for clarity.

Phase Behavior of S/I−TD. Figure 2 shows SAXS patterns for a PS-poor diblock, S/I 8/26, diluted with varying levels of TD. All patterns were acquired above the PS-rich domain T_g and 5−25 °C below the order−disorder transition (ODT) temperature (T_{ODT}, as discussed further below). The bulk diblock shows SAXS peaks in a q/q^* ratio of $1:\sqrt{3}:\sqrt{4}...$, characteristic of the hexagonally packed cylinders of PS (C_S) expected for this composition.[33] The more diluted systems shown in Figure 2 exhibit peaks in a q/q^* ratio of $1:\sqrt{2}:\sqrt{3}$, characteristic of a body-centered-cubic (bcc) packing of spheres; from the diblock's composition and the preference of TD for the PI-rich regions, we infer that the spheres are the PS-rich domains (S_S). At a weight fraction of polymer $W_P = 0.806$, the C_S morphology is observed at 93 °C and below, while the S_S morphology is observed from 96 °C up to T_{ODT}. This order−order transition (OOT) was fully thermoreversible in less than 10 min (the time allotted for equilibration prior to acquiring SAXS data).

Figure 3 shows comparable SAXS data taken on TD solutions of a PS-rich diblock, S/I 19/7, which has a bulk morphology of hexagonally packed cylinders of PI (C_I). With increasing TD addition, the structure first transforms to a PI-poor gyroid structure (G_I), as reflected by the peaks in a q/q^* ratio of $1:\sqrt{4/3}$; then to a lamellar structure (L), with $q/q^* = 1:2:3$; then to a PS-poor gyroid structure (G_S); and then to the C_S structure, exactly the same sequence observed in bulk S/I diblocks near the ODT as the isoprene fraction is increased.[33] Further dilution of this diblock with TD did not lead to an ordered array of spheres (S_S), but rather a disordered

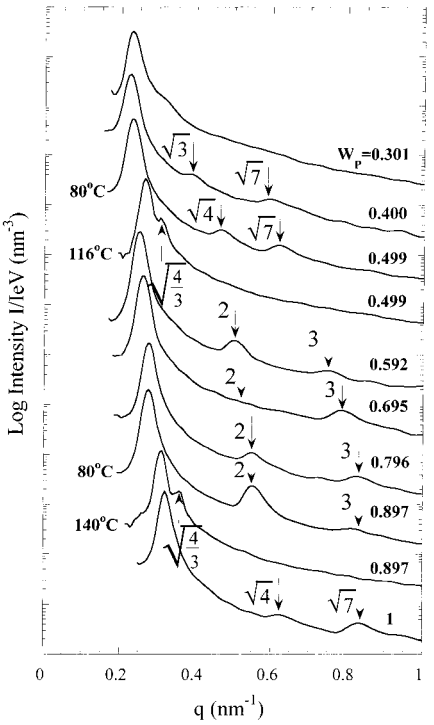

Figure 3. SAXS patterns for TD solutions of S/I 19/7 at various polymer weight fractions W_P. From bottom (bulk diblock) to top (most dilute solution), mesophase morphologies (W_P, T) are: C_I (1, 140 °C); G_I (0.897, 140 °C); L (0.897, 80 °C); L (0.796, 90 °C); L (0.695, 80 °C); L (0.592, 80 °C); G_S (0.499, 116 °C); C_S (0.499, 80 °C); C_S (0.400, 80 °C); micellar (0.301, 100 °C). Arrows indicate the positions of higher-order reflections characteristic of the mesophase structure. Profiles are shifted along the intensity axis for clarity.

micellar structure, at least at higher temperatures; the SAXS pattern from this structure, shown as the uppermost curve in Figure 3, can be quantitatively described by models for liquidlike packing of hard core−corona spheres.[27,34] For solutions exhibiting the L phase, the relative intensities of the higher-order peaks change as the volume fraction of PS-rich lamellae decreases through $^1/_2$ as TD is progressively added; the absence of a discernible second-order peak for the $W_P = 0.695$ solution indicates that the PS-rich and PI-rich lamellae should have nearly equal thicknesses, in good agreement with a volume fraction of the PS-rich domains of 0.485 calculated using the room temperature densities of PS, PI, and TD, assuming no volume change of mixing and taking the PS-rich domains to contain 8 wt % TD. The solution with $W_P = 0.897$ exhibits the L phase at lower temperatures, transforming to the G_I structure on heating, while the solution with $W_P = 0.499$ exhibits the C_S phase at lower temperatures, transforming to the G_S phase on heating. The OOTs evident in Figure 3 were also found to be fully thermoreversible and rapid.

Figure 4 shows selected SAXS patterns, taken during heating, for a TD solution of S/I 19/7 with $W_P = 0.513$. As with the $W_P = 0.499$ solution, the low-temperature morphology is C_S, which transforms to G_S on raising the temperature from 94 to 96 °C. On further heating to 124 °C, the higher-order peaks disappear, and the primary peak broadens significantly, reflecting the ODT. Figure 5 shows how the primary peak position q^* and the primary peak full width at half-maximum intensity ($W_{1/2}$) change with temperature. The C_S−G_S OOT is clearly revealed by a small shift in both q^* and $W_{1/2}$ at

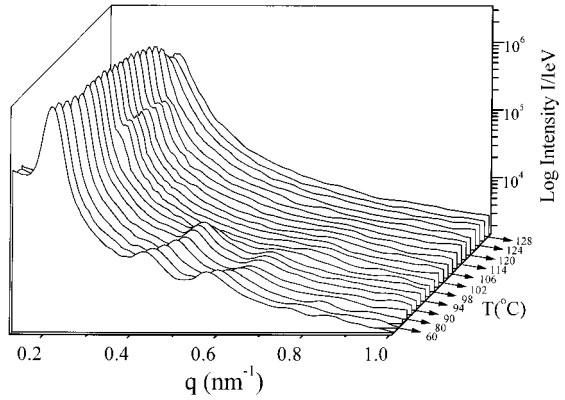

Figure 4. SAXS profiles acquired for S/I 19/7−TD (W_P = 0.513) on heating. The morphology changes from C_S to G_S to D (disordered) during heating.

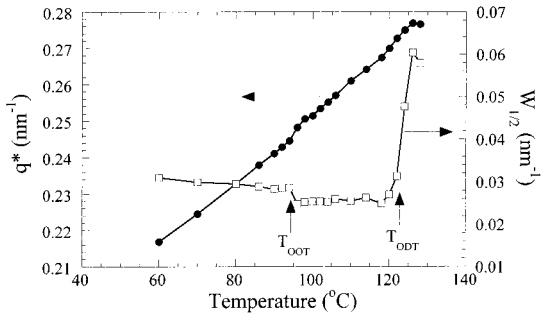

Figure 5. q^* (●, left axis) and $W_{1/2}$ (□, right axis) for S/I 19/7−TD (W_P = 0.513) on heating, showing a $C_I \rightarrow G_I$ OOT at 95 °C and the $G_I \rightarrow$ D ODT at 124 °C.

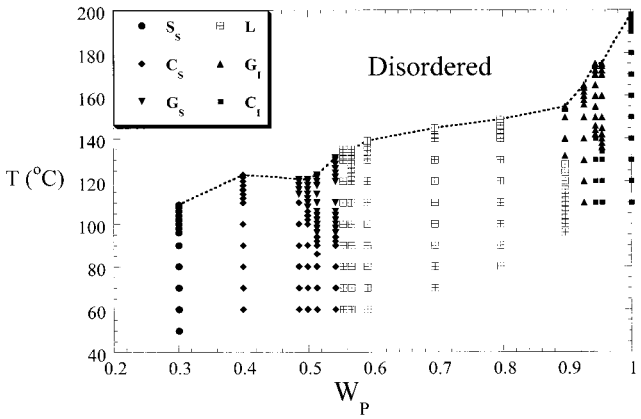

Figure 6. S/I 19/7−TD phase diagram. Bulk diblock (W_P = 1) is represented on the right axis. Mesophase morphologies are distinguished by different symbols (see key). All data points correspond to temperatures above the PS-rich domain T_g. Dotted line connects points on the ODT locus.

95 °C, while the sharp increase in $W_{1/2}$ at 124 °C signifies the ODT.[35] Subsequent thermoreversibility tests repeatedly recovered the C_S and G_S mesophases in the appropriate temperature ranges, strongly suggesting that the observed OOT is a transition between equilibrium phases.

Variable-temperature SAXS experiments analogous to those in Figure 4, but for TD solutions with various W_P, were used to generate the phase diagram for S/I 19/7−TD shown in Figure 6. All ODTs and OOTs were located with a precision of ±2 °C or better. Figure 6 has both similarities with, and differences from, the phase diagrams presented by Hanley et al.[24] for a PS-poor S/I diblock in the PS-selective solvents DEP and DBP−

roughly speaking, the inverse of the system in Figure 6. In both cases, T_{ODT} decreases nearly monotonically with increasing dilution: rapidly at first and then appearing to plateau at lower W_P. This behavior mimics that shown for the PS domain T_g in Figure 1, where solvent initially partitions into both PS-rich and PI-rich domains (thus screening interactions between S and I), but eventually a solubility limit for TD in the PS-rich phase is reached. Figure 6 clearly shows that both gyroid phases (G_I and G_S) exist only as "bubbles" close to the ODT line; on cooling, these gyroid structures transform reversibly to either cylinders or lamellae, depending on the precise solution concentration. The same phase diagram topology is predicted for block copolymer melts, where the G phases are calculated to "pinch off" (in favor of C or L) as the segregation strength is increased.[18] This prediction has been difficult to verify for melts, whose phase transformation dynamics can be quite sluggish at the necessary segregation strengths,[36] but the limited temperature range of both G phases is clearly evident in our concentrated solutions.

We recognize that this analogy should not be taken at face value: melts and solutions are not entirely equivalent. The possibility for solvent to accumulate preferentially at the interstices between cylinders (where three hexagonal unit cells meet), shown experimentally for lipid−oil systems,[37] tends to stabilize C phases. This effect may be a factor in the asymmetry observed in Figure 6, where the G_S phase (lower W_P, higher solvent content) transforms to C_S on cooling at all compositions, while the G_I phase (higher W_P, lower solvent content) transforms to either C_I or L, depending on composition. However, preferential solvent accumulation will not stabilize L vs G, so the observation of a $G_I \rightarrow L$ transition on cooling for even one composition suggests that nonuniform solvent distribution is not the only factor restricting the G phases to near the ODT. Finally, close inspection of Figure 6 shows that the G-phase solutions exhibit T_{ODT} values slightly but systematically below those predicted by smoothly connecting the T_{ODT} values for the compositionally adjacent mesophases. This effect was consistently observed in all solutions that showed either G phase and suggests that fluctuations (absent in mean-field theoretical treatments) have a stronger effect on the stability of the G structure than on L or C. Such a subtle effect is difficult to detect in the usual melt phase map, because of the difficulty in matching diblock molecular weights precisely during synthesis, though this effect can be seen on close examination of phase diagrams constructed by blending two similar diblocks across the G region.[36]

With the exception of the G "bubbles", the phase boundaries in Figure 6 are nearly vertical (in particular, note the region around $W_P = 0.55$, where the C/L boundary is vertical to within ± 0.006 in W_P over its entire extent, 33 °C). This is a consequence of the strong selectivity of TD for PI at all temperatures; little change in solvent partitioning (and thus in the volume fractions of the PS-rich and PI-rich domains) occurs as temperature is varied, unlike DEP and other less strongly selective solvents where the solvent becomes more neutral as temperature is increased. Diagrams analogous to Figure 6 for TD solutions of the other nine diblocks listed in Table 1 may be found elsewhere[38] and are summarized below. Though numerous OOTs involving the G_I or G_S phases were found in the TD solutions studied in this work, only two other OOTs were observed. For S/I 24/6 at $W_P = 0.520$, a direct C_S to L transition was observed on heating, with no intervening G_S phase. This transition is "reversed" from that for melts, where L to C_S is predicted[33] and observed[5] on heating. Though a reduction in solvent selectivity with increased temperature could be responsible for this "reversed" OOT, we note that the solution composition is very close to the $C_S/G_S/L$ triple point (as is the S/I 19/7 solution with $W_P = 0.55$ discussed above), and so the unusual nature of this OOT could also be due to a slightly nonuniform distribution of solvent in the C_S phase, as discussed above. The other OOT observed is that shown in Figure 2 for S/I 8/26 at $W_P = 0.806$, from C_S to S_S on heating. This transition is in the direction predicted theoretically and observed experimentally for S/I diblock melts.[4] If the transition were induced by a reduction in solvent selectivity with increased temperature, the phase boundary would have the reverse slope, i.e., S_S to C_S on heating.

In DEP, Hanley et al.[24] observed a substantial region of coexistence between the L and C phases, extending over as much as 0.05 in W_P or 30 °C in temperature. We did not observe coexistence in any of our solutions (in any solvent), though we used very small increments in W_P and T near phase boundaries in an attempt to do so, as well as checking the thermoreversibility of the phase transitions. Though coexistence of two phases in these two-component solutions is allowed by the Gibbs phase rule, any coexistence in our solutions must be restricted to very small regions between our measurement points (spacing typically 0.015 in W_P, or 2 °C, in the vicinity of a phase boundary; temperature uniformity in the SAXS cell is ±1 °C, so finer temperature increments cannot be probed).

Finally, none of our solutions (in any solvent) exhibited a definitive face-centered-cubic (fcc) packing of spheres, though this morphology was found for some S/I diblock solutions in DEP by Hanley et al.[24] and in decane by McConnell et al.[17,23] In particular, our solutions of S/I 8/17, 11/10, and 17/9 in TD showed the bcc structure in concentration regions where McConnell et al.[17,23] found that similar polymers in decane formed fcc spheres. The origin of these discrepancies remains unclear, though we note our experience that solutions must be annealed above the T_g of the PS domains to achieve the equilibrium structure.

Composite Phase Map of S/I−TD. All the observations noted in the preceding section suggest that the phase diagrams for our TD solutions can be constructively interpreted using the well-known concepts from melt phase maps, considering the solvent to merely "add" to the domains formed by one block. If true, then it may be possible to collapse the phase diagrams for TD solutions of all our S/I diblocks together in a simple two-dimensional plot of segregation strength vs composition. The most directly accessible composition parameter is the weight fraction of polystyrene in the solution, W_{PS}. An appropriate surrogate for segregation strength is less obvious, as there are three relevant interaction parameters in the system (PS−PI, PS−TD, PI−TD) and the solvent content varies (so, in fact, the true phase space is three-dimensional,[20] not two-dimensional). To proceed, we take as a crude first approximation that the segregation strength of the TD solutions is the same as that of the melts of the diblocks they contain. On the basis of the T_{ODT} values[38] for three PS-poor S/I diblocks

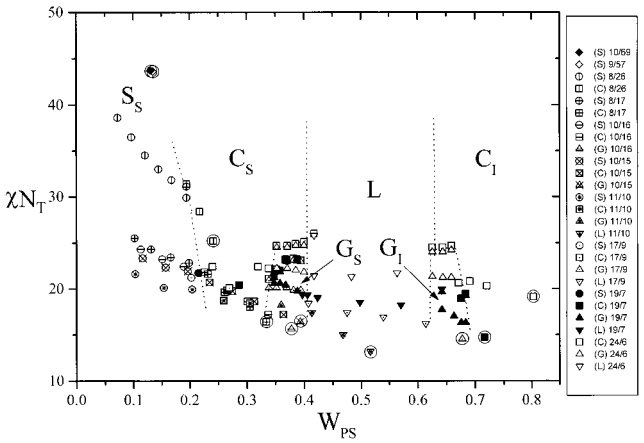

Figure 7. Composite S/I−TD phase map, constructed from phase diagrams for 10 individual S/I diblocks in TD. Abscissa (W_{PS}) is the weight fraction of polystyrene in solution. ODTs are represented by a single symbol; circled symbols correspond to the 10 melts. Thermotropic OOTs are denoted by two overlapping points at identical W_{PS} and slightly different χN_T. Key to the right of the figure indicates the identity of each solution. Shapes of the symbols represent different mesophases: C (squares), G (upward-pointing triangles), L (downward-pointing triangles), and S (circles and diamonds). Different diblocks are coded by the mark inside each symbol. Approximate phase boundaries are indicated by dotted lines.

of nearly identical composition and known molecular weight, including S/I 10/69 and 9/57, we obtain

$$\chi_{PS-PI} = -0.0522 + 48.8/T \text{ (K)} \qquad (1)$$

This expression takes as its reference the volume occupied by one S residue, at the temperature of interest. Using the χ_{PS-PI} relation in eq 1 and the total degree of polymerization N_T calculated from the molecular weights in Table 1, a value of χN_T for each solution was calculated at the relevant ODT or OOT temperature.

Figure 7 shows the composite phase map for the S/I−TD system. In this work, ODTs were located for 10 melts and 78 solutions with assigned $\chi N_T < 50$; each of these 88 ODTs is represented by a single symbol in Figure 7. The circled symbols correspond to the 10 melts and trace out the familiar form of the diblock melt ODT curve.[18,33] We also located 21 thermotropic OOTs in the solutions (18 of these at C/G boundaries), which are each denoted by two overlapping points at identical W_{PS} and slightly different χN_T. Surprisingly, this simple approach collapses the data reasonably well; clearly-defined boundaries between S_S/C_S, C_S/L, and L/C_I are indicated with dashed, near-vertical lines, while the G_I and G_S phases are restricted to small bubbles near the ODT. Indeed, over the midrange of the map ($0.3 < W_{PS} < 0.7$), the data collapse reasonably well vertically (in χN_T) as well as horizontally (in W_{PS}). This apparent vertical collapse is largely a consequence of the similarity of *all* the estimated χN_T values in this region (15−22 for the solution ODTs), which in turn results from two factors: the modest reduction in T_{ODT} upon dilution with TD (so that solutions and melts of the same diblock have similar estimated χN_T) and the modest variation in χN_T for the melt phase map over its midrange, as evident in the locus described by the melt data (circled symbols). The breakdown of this simple superposition scheme is evident at low W_{PS}; while solutions prepared from a given diblock show the correct trend in $(\chi N_T)_{ODT}$ upon dilution (an increase as $W_{PS} \rightarrow 0$), they do not quantitatively superpose onto the melt phase map. Finally, we note that the density differences between PS, PI, and TD would lead to slight shifts of the phase boundaries if compositions were gauged by volume fraction (ϕ_{PS}) rather than weight fraction. Maps constructed with ϕ_{PS} as the abscissa, calculated under the assumptions of perfect solvent selectivity and no volume change of mixing, may be found elsewhere;[38] while the higher density of PS causes the phase boundaries to occur at lower values of ϕ_{PS} than W_{PS}, the degree of collapse is equally good with either parameter given the finite number of data points.

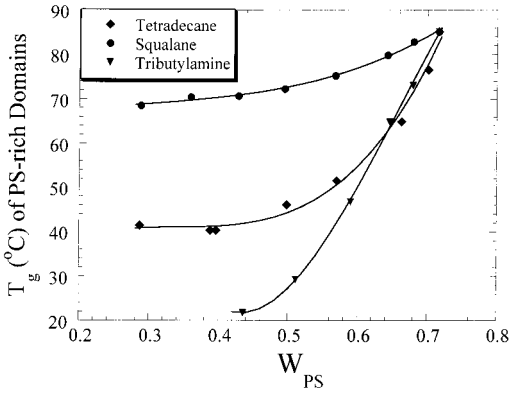

Figure 8. Glass transition temperatures (T_g) for the PS-rich domains in solutions of S/I 19/7 in squalane (●), tetradecane (◆), and tributylamine (▼). Abscissa (W_{PS}) is the weight fraction of PS in the solution; the rightmost point (common to all three sets) corresponds to the undiluted diblock. Continuous curves are guides to the eye.

Solvent Selectivity. The simplicity of Figure 7 prompted us to ask whether this map might be characteristic of all strongly selective solvents, i.e., those that are nonsolvents for one block and good solvents for the other, or whether substantial differences could still exist within this group. We thus complemented TD with two other solvents, squalane (SQ) and tributylamine (TBA), both of which are nonsolvents for polystyrene but good solvents for polyisoprene. The values of the PS-rich domain T_g for solutions of S/I 19/7 in these three solvents are shown in Figure 8. While differences in the plasticizing efficiency of different solvents (e.g., T_g of solvent required in Fox equation) can produce differences in T_g at a fixed solvent content, the large differences seen in Figure 8 clearly reflect a difference in solvent partitioning, with the selectivity going in the order SQ > TD > TBA.

Differences in selectivity should be reflected in the location of the phase boundaries as well.[24] A true neutral solvent should produce solutions having the same mesophase as the melt (except perhaps when the melt has a composition such that a thermotropic OOT occurs for some χN_T). Thus, the closer a solvent is to neutrality, the more diluted the polymer must be to cross a particular lyotropic phase boundary. Figure 9 shows the phase diagram constructed for S/I 19/7−TBA solutions. The vertical bars at the top of the diagram indicate the locations of the dilution-induced transitions when the solvent is TD (intersections of the OOT loci with the ODT curve, taken from Figure 6; ODT curve for TD solutions is shown in Figure 9 as dotted line). Comparison of the mesophase stability limits in the two solvents shows that the transitions occur at higher

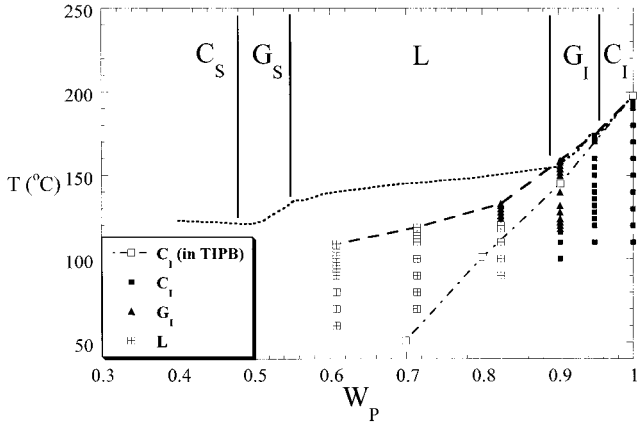

Figure 9. S/I 19/7−TBA phase diagram. Bulk diblock (W_P = 1) is represented on the right axis. Mesophase morphologies are distinguished by different symbols (see key). All data points correspond to temperatures above the PS-rich domain T_g. Dashed line connects points on the ODT locus; dotted line is the ODT locus for the same diblock in TD solution. For comparison, regions of stability of the different mesophases for S/I 19/7 in TD at the ODT locus are shown between vertical bars at the top of the figure. Open squares and dot−dashed line correspond to solutions of S/I 19/7 in the neutral solvent TIPB.

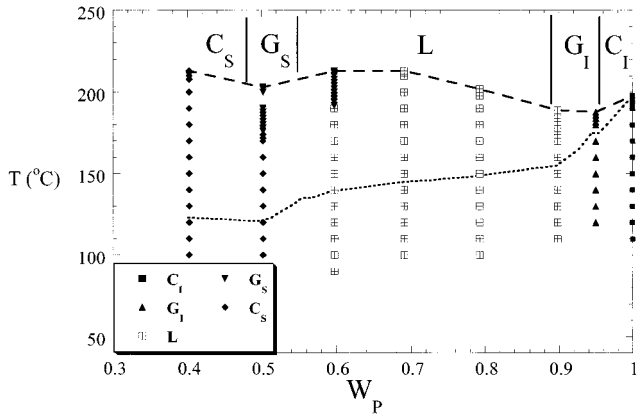

Figure 10. S/I 19/7−SQ phase diagram. Bulk diblock (W_P = 1) is represented on the right axis. Mesophase morphologies are distinguished by different symbols (see key). All data points correspond to temperatures above the PS-rich domain T_g. Dashed line connects points on the ODT locus; dotted line is the ODT locus for the same diblock in TD solution. For comparison, regions of stability of the different mesophases for S/I 19/7 in TD at the ODT locus are shown between vertical bars at the top of the figure.

dilutions (lower W_P) when TBA is employed and that the ODT curve for the TBA solutions (dashed curve) lies significantly below that for the TD solutions. These two observations clearly point to TBA being less selective than TD, as inferred from the PS domain T_g values. The consistency between these two methods for evaluating selectivity—DSC at the PS-rich domain T_g (T < 80 °C) and phase boundary location (T > 110 °C)—demonstrates that (as expected) no inversion of selectivity occurs with temperature over the relevant range. For comparison, Figure 9 also shows T_{ODT} values for S/I 19/7 in a neutral solvent: triisopropylbenzene (TIPB). In TIPB, the mesophase remains C_I for all concentrations examined, and T_{ODT} falls off comparatively rapidly upon dilution. Using the χ_{PS-PI} expression presented in eq 1 and assuming that the effective segmental interaction parameter in solution (χ_{eff}) obeys[10]

$$\chi_{eff} = \chi_{PS-PI}\phi_P^{-\alpha} \qquad (2)$$

we find that $\alpha \approx 1.5$, in satisfactory agreement with the blob model prediction[39,40] of $\alpha = 1.6$. Values of α determined experimentally in neutral solvents[10] vary from 1.2 to 1.6, but we note that the value of α depends sensitively on the inverse temperature coefficient in the expression for χ_{PS-PI}. The temperature dependence of χ_{PS-PI} is much more difficult to determine precisely than the magnitude of χ_{PS-PI} at any given temperature; indeed, even for the well-studied PS−PI system, very different expressions for χ_{PS-PI} have been presented, though their magnitudes are similar.[41]

Figure 10 shows the analogous diagram for solutions of the same diblock in SQ. When S/I 19/7 is diluted with SQ, phase boundaries are crossed slightly earlier (higher W_P) than when TD is employed, indicating that SQ is slightly more selective than TD, again consistent with the conclusions from DSC. Qualitatively, it is unsurprising that SQ is a poorer solvent than TD for PS, given its higher molecular weight (423 vs 198 g/mol) and more branched structure (higher density of methyl groups, lower solubility parameter). However, the differences in the locations of the lyotropic order−order transitions between SQ and TD solutions are modest, and a composite map[8] analogous to Figure 7 can be constructed for S/I−SQ solutions with nearly as good superposition (though we examined far fewer SQ than TD solutions). This observation suggests that for very strongly selective solvents, such as TD and SQ, the melt phase map does indeed provide a useful, semiquantitative guide in determining the content of solvent required to produce a given mesophase.

However, important differences between TD and SQ can be seen as well, principally in the ODT loci shown in Figure 10. In SQ, the ODT curve is elevated relative to that found for TD solutions, consistent with SQ being more selective than TD. But interestingly, most of the S/I 19/7 solutions in SQ (including the one containing only 40% polymer) actually show T_{ODT} values *higher* than that for the undiluted melt. That an ordered structure in an all-hydrocarbon block copolymer can be *stabilized* by the addition of a hydrocarbon solvent is remarkable, since all the components have relatively weak dispersive interactions with each other. This effect is even more dramatic for SQ solutions of S/I 24/6, as shown in Figure 11. This polymer forms the C_I phase in bulk; when the diblock is diluted sufficiently to produce the mirror-image C_S phase, the ODT has actually been *elevated* by 80 °C. Supercritical CO_2 has been shown to induce ordering in a polystyrene−poly(*n*-butyl methacrylate) diblock,[42] but that system is unusual in that the interblock segregation strength *increases* with temperature; for S/I diblocks, both supercritical CO_2 and ethane produce the usual T_{ODT} depression.[43]

Two factors contribute to this T_{ODT} elevation. The first is the shape of the diblock melt phase map, as traced out by the circled points in Figure 7. Bulk S/I 19/7 and 24/6 lie on the high-W_{PS} side of the symmetry point; if we consider the addition of a very strongly selective solvent to correspond to a horizontal movement on the phase map of Figure 7 (implicit in the simple approach that we have used to assign χN_T values for the solutions in Figure 7), then one would expect that T_{ODT} should increase upon dilution until the symmetry point of the phase map is reached. The converse of this argument

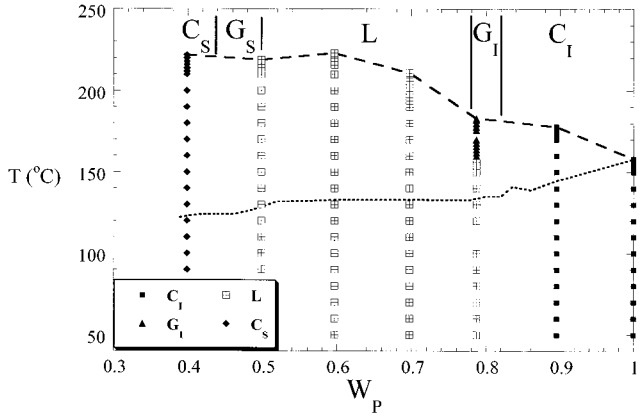

Figure 11. S/I 24/6−SQ phase diagram. Bulk diblock ($W_P = 1$) is represented on the right axis. Mesophase morphologies are distinguished by different symbols (see key). All data points correspond to temperatures above the PS-rich domain T_g. Dashed line connects points on the ODT locus; dotted line is the ODT locus for the same diblock in TD solution. For comparison, regions of stability of the different mesophases for S/I 24/6 in TD at the ODT locus are shown between vertical bars at the top of the figure.

suggests that this elevation of T_{ODT} would be absent if one were to start with a diblock on the PS-poor side of the phase map, and indeed, SQ solutions of the two diblocks in Table 1 with bulk $W_S \approx 0.13$ *do* show a monotonic reduction of T_{ODT} upon dilution.[38] However, the shape of the melt phase map alone is insufficient to explain the higher T_{ODT} for the C_S-phase solution than for the C_I-phase solution in Figure 11, since these lie approximately equal distances in either direction from the center of the map. Rather, this asymmetry is a consequence of the fact that SQ is an *extremely* poor solvent for PS, evidently worse even than the PI blocks of the diblock. Clearly, even among strongly selective—and chemically similar—solvents such as TD and SQ, significant quantitative differences in the diblock−solvent phase behavior can be present.

Finally, we note that the addition of solvent can substantially alter not only the structure of the mesophase but also its characteristic domain spacing; our findings on this subject will be presented in a subsequent paper.[44]

Conclusions

The addition of strongly selective solvents can greatly enrich the phase behavior of block copolymers, producing a variety of lyotropic order−order transitions without severely depressing (and, in some cases, substantially elevating) the order−disorder transition temperature. Even among strongly selective solvents (those that are good solvents for one block, nonsolvents for the other), substantial differences in selectivity exist. These differences are rapidly gauged through measurement of the glass transition temperature of the polystyrene-rich domains and manifest themselves both in the concentrations at which lyotropic order−order transitions occur and in the locus of T_{ODT} vs concentration. The gyroid phases are stable over only limited regions near the ODT locus; thermoreversible and rapid order−order transitions to cylindrical or lamellar phases occur upon cooling. Though coexistence of different ordered phases is thermodynamically permitted in these two-component solutions, all our observations are consistent with a single structure at any solution composition and temperature, indicating that any coexistence regions in these concentrated solutions must be quite small. For the most strongly selective solvents (such as TD and SQ for S/I diblocks), the compositions for which the different mesophases are stable can be reasonably well predicted using the diblock melt phase map and simply considering the solvent to add to the fraction of the soluble block.

Acknowledgment. This work was supported by the Princeton Center of Complex Materials, a National Science Foundation Materials Research Science and Engineering Center (DMR-9400362 and DMR-9809483). We are most grateful to Dr. Gary R. Marchand for the synthesis of several of these diblocks at DEXCO Polymers.

References and Notes

(1) Bates, F. S.; Fredrickson, G. H. *Annu. Rev. Phys. Chem.* **1990**, *41*, 525.
(2) Hamley, I. W. *The Physics of Block Copolymers*; Oxford University Press: Oxford, 1998.
(3) Almdal, K.; Koppi, K.; Bates, F. S.; Mortensen, K. *Macromolecules* **1992**, *25*, 1743.
(4) Sakurai, S.; Kawada, H.; Hashimoto, T.; Fetters, L. J. *Macromolecules* **1993**, *26*, 5796.
(5) Hajduk, D. A.; Gruner, S. M.; Rangarajan, P.; Register, R. A.; Fetters, L. J.; Honeker, C.; Albalak, R.; Thomas, E. L. *Macromolecules* **1994**, *27*, 490.
(6) Koppi, K.; Tirrell, M.; Bates, F. S.; Almdal, K.; Mortensen, K. *J. Rheol.* **1994**, *38*, 999.
(7) Förster, S.; Khandpur, A. K.; Zhao, J.; Bates, F. S.; Hamley, I. W.; Ryan, A. J.; Bras, W. *Macromolecules* **1994**, *27*, 6922.
(8) Gallot, B. In *Liquid Crystalline Order in Polymers*; Blumstein, A., Ed.; Academic Press: New York, 1978; Chapter 6.
(9) Lodge, T. P.; Hamersky, M. W.; Hanley, K. J.; Huang, C.-I. *Macromolecules* **1997**, *30*, 6139.
(10) Lodge, T. P.; Pan, C.; Jin, X.; Liu, Z.; Zhao, J.; Maurer, W. W.; Bates, F. S. *J. Polym. Sci., Part B: Polym. Phys.* **1995**, *33*, 2289.
(11) Huang, C.-I.; Chapman, B. R.; Lodge, T. P.; Balsara, N. P. *Macromolecules* **1998**, *31*, 9384.
(12) Handlin, D. L., Jr. U.S. Patent 4,798,853, issued Jan 20, 1987, to Shell Oil Company.
(13) Soenen, H.; Berghmans, H.; Winter, H. H.; Overbergh, N. *Polymer* **1997**, *38*, 5653.
(14) Laurer, J. H.; Mulling, J. F.; Khan, S. A.; Spontak, R. J.; Bukovnik, R. *J. Polym. Sci., Part B: Polym. Phys.* **1998**, *36*, 2379.
(15) Watanabe, H.; Kotaka, T.; Hashimoto, T.; Shibayama, M.;. Kawai, H. *J. Rheol.* **1982**, *26*, 153.
(16) Halperin, A. *Macromolecules* **1987**, *20*, 2943.
(17) McConnell, G. A.; Gast, A. P.; Huang, J. S.; Smith, S. D. *Phys. Rev. Lett.* **1993**, *71*, 2102.
(18) Matsen, M. W.; Bates, F. S. *Macromolecules* **1996**, *29*, 1091.
(19) Banaszak, M.; Whitmore, M. D. *Macromolecules* **1992**, *25*, 3406.
(20) Huang, C.-I.; Lodge, T. P. *Macromolecules* **1998**, *31*, 3556.
(21) Alexandridis, P.; Olsson, U.; Lindman, B. *Langmuir* **1998**, *14*, 2627.
(22) Shibayama, M.; Hashimoto, T.; Kawai, H. *Macromolecules* **1983**, *16*, 16.
(23) McConnell, G. A.; Gast, A. P. *Macromolecules* **1997**, *30*, 435.
(24) Hanley, K. J.; Lodge, T. P.; Huang, C.-I. *Macromolecules* **2000**, *33*, 5918.
(25) Sebastian, J. M.; Register, R. A. *J. Appl. Polym. Sci.* **2001**, *82*, 2056.
(26) Register, R. A.; Bell, T. R. *J. Polym. Sci., Part B: Polym. Phys.* **1992**, *30*, 569.
(27) Adams, J. L.; Quiram, D. J.; Graessley, W. W.; Register, R. A.; Marchand, G. R. *Macromolecules* **1996**, *29*, 2929.
(28) Sebastian, J. M. Ph.D. Thesis, Princeton University, 2001.
(29) Fox, T. G. *Bull. Am. Phys. Soc.* **1956**, *1*, 123.
(30) Boyer, R. F. *J. Appl. Phys.* **1954**, *25*, 825.
(31) Chow, T. S. *Macromolecules* **1980**, *13*, 362.
(32) Soenen, H.; Liskova, A.; Reynders, K.; Berghmans, H.; Winter, H. H.; Overbergh, N. *Polymer* **1997**, *38*, 5661.

(33) Khandpur, A. K.; Förster, S.; Bates, F. S.; Hamley, I. W.; Ryan, A. J.; Bras, W.; Almdal, K.; Mortensen, K. *Macromolecules* **1995**, *28*, 8796.
(34) Kinning, D. J.; Thomas, E. L. *Macromolecules* **1984**, *17*, 1712.
(35) Wolff, T.; Burger, C.; Ruland, W. *Macromolecules* **1993**, *26*, 1707.
(36) Lai, C.; Russel, W. B.; Register, R. A.; Marchand, G. R.; Adamson, D. H. *Macromolecules* **2000**, *33*, 3461.
(37) Turner, D. C.; Gruner, S. M.; Huang, J. S. *Biochemistry* **1992**, *31*, 1356.
(38) Lai, C. Ph.D. Thesis, Princeton University, 1999.
(39) Olvera de la Cruz, M. *J. Chem. Phys.* **1989**, *90*, 1995.
(40) Fredrickson, G. H.; Leibler, L. *Macromolecules* **1989**, *22*, 1238.
(41) Adams, J. L.; Graessley, W. W.; Register, R. A. *Macromolecules* **1994**, *27*, 6026.
(42) Watkins, J. J.; Brown, G. D.; RamachandraRao, V. S.; Pollard, M. A.; Russell, T. P. *Macromolecules* **1999**, *32*, 7737.
(43) Vogt, B. D.; Brown, G. D.; RamachandraRao, V. S.; Watkins, J. J. *Macromolecules* **1999**, *32*, 7907.
(44) Lai, C.; Russel, W. B.; Register, R. A. *Macromolecules*, to be submitted.

MA011696Z